tvst

Article

Contrast Sensitivity and Equivalent Intrinsic Noise in X-Linked Retinoschisis

J. Jason McAnany[1,2], Jason C. Park[1], Gerald A. Fishman[1,3], and Robert A. Hyde[1]

[1] Department of Ophthalmology and Visual Sciences, University of Illinois at Chicago, Chicago, IL, USA
[2] Department of Bioengineering, University of Illinois at Chicago, Chicago, IL, USA
[3] The Pangere Center for Inherited Retinal Diseases, The Chicago Lighthouse, Chicago, IL, USA

Correspondence: J. Jason McAnany, University of Illinois at Chicago, Department of Ophthalmology and Visual Sciences, 1855 W. Taylor St., MC/648, Chicago, IL 60612, USA.
e-mail: jmcana1@uic.edu

Received: November 30, 2021
Accepted: February 10, 2022
Published: March 8, 2022

Keywords: psychophysics; retinal degeneration; noise; contrast sensitivity

Citation: McAnany JJ, Park JC, Fishman GA, Hyde RA. Contrast sensitivity and equivalent intrinsic noise in X-linked retinoschisis. Transl Vis Sci Technol. 2022;11(3):7, https://doi.org/10.1167/tvst.11.3.7

Purpose: To define relationships among contrast sensitivity (CS), equivalent intrinsic noise (N_{eq}; a measure of noise within the visual pathway), and retinal thickness in X-linked retinoschisis (XLRS).

Methods: Nine XLRS and 10 visually-normal subjects participated. CS was measured in the presence and absence of luminance noise. These data were fit with a standard model to estimate N_{eq} and sampling efficiency (an estimate of the ability to use stimulus information). Optical coherence tomography images were obtained to quantify outer nuclear layer (ONL^+) and outer segment (OS^+) thickness. A linear structure-function model was used to describe the relationship between CS and the product of ONL^+ and OS^+ thickness.

Results: CS in the absence of noise (CS_0) for the XLRS subjects ranged from normal to as much as 1.5× below the lower limit of normal. Four of the nine subjects with XLRS had abnormally high N_{eq}, whereas two others had sampling efficiency that was borderline abnormal. Log CS_0 for the subjects with XLRS was correlated significantly with log N_{eq} ($r = -0.78$, $P = 0.01$), but not with log efficiency ($r = 0.19$, $P = 0.63$). CS_0 and N_{eq}, but not efficiency, conformed to the linear $ONL^+ \times OS^+$ structure-function model.

Conclusions: The XLRS subjects in this study who had elevated internal noise had abnormally low CS; both internal noise and CS fell within the predicted limits of a structure-function model.

Translational Relevance: Internal noise measurements can provide insight into a source of CS loss in some individuals with XLRS.

Introduction

X-linked retinoschisis (XLRS) is caused by mutations in the *Retinoschisin 1* (*RS1*) gene and is one of the most common juvenile onset vitreoretinal degenerative diseases.[1–4] The fundus of patients with XLRS is characterized by spoke-wheel-like cystic changes within the foveal region. A peripheral retinoschisis can also be observed, most frequently in the temporal retina.[3] In addition to the spoke-wheel-like pattern of cysts noted on a clinical fundus examination, optical coherence tomography (OCT) imaging can show inner-retina schisis and thinning of the photoreceptor layer.[5] The most common initial clinical presentation is reduced visual acuity (VA), often by 10 years of age.[6] Although VA is not correlated with cystic cavity volume[7] or total retinal thickness,[5] there is a correlation with photoreceptor outer segment thickness.[5]

In addition to VA loss, there are reports of contrast sensitivity (CS) reductions in individuals with XLRS that have been measured using both sinewave grating targets[8] and letters.[7,8] CS quantifies the ability to discern differences in luminance, most commonly measured under photopic conditions, and is an essential aspect of visual function. Contrast processing forms the basis for the perception of objects and CS losses are correlated with difficulty in performing tasks of daily living.[9,10] Studies in subjects with XLRS have shown that the extent of CS loss is dependent on the characteristics of the stimulus. For

example, sensitivity for low spatial frequency gratings,[8] large letters,[7,8] and diffuse full-field flashes[11] may be normal or only mildly reduced, whereas CS for moderate to high frequency sinewave gratings can be reduced substantially.[8] The factors that underlie CS loss in subjects with XLRS, when present, are uncertain.

One potential explanation for the reduced CS comes from single cell recordings in *Rs1* mutant mice, which have elevated background activity ("noise").[12] Specifically, single cell recordings from retinal ganglion cells (RGCs) showed elevated spontaneous RGC activity in young *Rs1* mice compared to wild type mice.[12] The elevated spontaneous activity resulted in a decreased signal-to-noise ratio, which is anticipated to reduce sensitivity. Consistent with this finding, it has been proposed that a number of retinal diseases can be characterized by high levels of noise within the visual pathway,[13] which was supported by measurements in subjects with retinitis pigmentosa[14] and diabetic retinopathy.[15]

Studies of noise in visually-normal individuals and in patients with visual dysfunction have used the "equivalent input noise method" to noninvasively estimate the amount of noise within the visual pathway.[13–18] With this approach, CS measurements are made in the presence and absence of additive white luminance noise. These measurements are then analyzed using a model of human performance in noise, such as the linear amplifier model (LAM).[19] The LAM factors performance into two independent components: (1) equivalent intrinsic noise, which is an estimate of the amount of noise within the visual pathway; (2) sampling efficiency, which represents the subject's ability to optimally utilize stimulus information.[19]

In the present study, CS was measured in subjects with XLRS against a uniform field and in the presence of different levels of white spatial luminance noise. The LAM was used to estimate equivalent intrinsic noise and sampling efficiency. These data were compared to those obtained from visually-normal control subjects. Additionally, measures of equivalent intrinsic noise, sampling efficiency, and CS were compared to retinal thickness, obtained by OCT, to determine whether structural changes of the outer retina are associated with these psychophysical parameters.

Methods

Subjects

The study was approved by an institutional review board of the University of Illinois at Chicago and tenets of the Declaration of Helsinki were followed. All subjects provided written informed consent prior to participating. Nine unrelated male subjects with a clinical diagnosis of XLRS (ages 18 to 49 years) were recruited from the cohorts of the Chicago Lighthouse and the University of Illinois at Chicago, Illinois Eye and Ear Infirmary. These 9 subjects participated in a previous visual field perimetry study[20] and their clinical characteristics are described therein. In brief, the subjects with XLRS had typical fundus features, electroretinogram abnormalities, and VA loss. A mutation in the *RS1* gene was documented in each individual. Table lists the age, visual acuity,

Table. Subject characteristics

Subject No.	Color code	Age (yrs)	Acuity (log MAR)	Pelli-Robson CS	RS1 Variant	CAI treatment
1		18	0.52	1.85	c.214G>A (p.Glu72Lys)	Acetazolamide
2		19	0.68	1.85	c.218C>A (p.Ser73*)	No
3		21	0.58	1.75	Deletion of exons 1 – 5	No
4		25	0.36	1.95	Deletion of exon 2	No
5		34	0.56	1.75	c.578C>T (p.Pro193Leu)	No
6		35	0.60	1.75	c.422G>A (p.Arg141His)	Acetazolamide
7		37	0.66	1.80	c.208G>A (p.Gly70Ser)	No
8		40	0.40	1.75	c.208G>A (p.Gly70Ser)	No
9		49	0.60	1.75	c.286T>C (p.Trp96Arg)	No

Pelli-Robson chart CS, *RS1* mutation, and carbonic anhydrase inhibitor use at the time of testing. Ten visually-normal control subjects (six male and four female; ages 23 to 42 years) with no history of eye disease, normal distance VA, and normal CS assessed with the Pelli-Robson chart also participated in the study. Of note, there were no apparent differences in visual function (acuity, CS, internal noise, efficiency) between the male and female control subjects, so the male and female control data were combined for comparison to the male XLRS subject data. These control subjects also participated in the previous visual field perimetry study.[20] An independent samples t test indicated that the mean age of the controls (29 years) did not differ from that of the XLRS subjects (31 years) significantly ($t = 0.40$, $P = 0.69$).

Stimuli and Instrumentation

Stimuli were generated using a Cambridge Research Systems ViSaGe stimulus generator (Cambridge Research Systems, Ltd., Rochester, Kent, UK) and were displayed on a Mitsubishi Diamond Pro (2070) CRT monitor (Mitsubishi Electric Corp., Tokyo, Japan), as described elsewhere.[21,22] The monitor was viewed monocularly through a phoropter with the subject's optimal refractive correction. A 3.0 mm artificial pupil was mounted on the eyepiece of the phoropter to control retinal illuminance. The luminance values used to generate the stimuli were confirmed using a Minolta LS-110 photometer (Konica Minolta, Tokyo, Japan) and the temporal characteristics of the display were confirmed using an oscilloscope and photocell.

The test stimuli consisted of 10 letters from the Sloan set (C, D, H, K, N, O, R, S, V, Z) that were constructed according to published guidelines[23] and have been shown to have similar thresholds for measurements made in the presence and absence of luminance noise.[24] The letter size was equivalent to 1.4 log MAR (approximately 20/500 Snellen). Large letters were selected as test targets to ensure that the reduced visual acuity of the subjects with XLRS did not confound the CS measurements. In addition, letters are far more widely used in the clinic, as compared to sinewave grating targets. The disadvantage of large letter targets, however, is that letter CS loss in subjects with XLRS is more subtle than that measured with high frequency gratings.[8] The letter target was presented at the center of a uniform achromatic field (50 cd/m^2) or in a static noise field of the same mean luminance (the field covered an area that was approximately twice as large as the letter). The noise consisted of independently generated

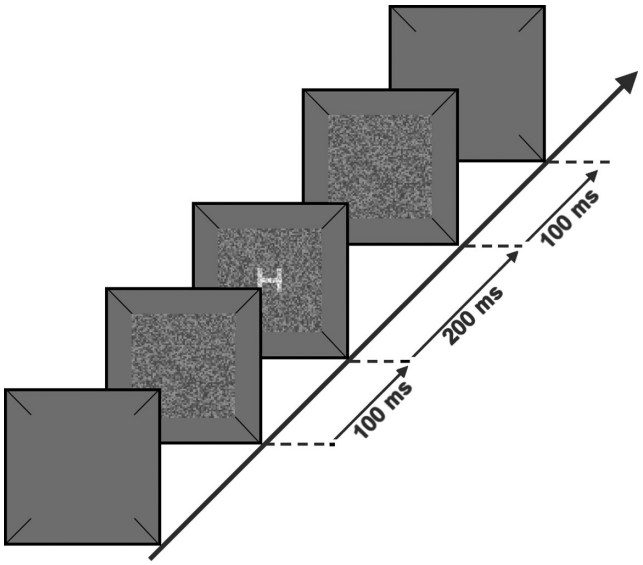

Figure 1. Schematic illustration of the sequence of stimulus presentation. A letter target was presented for 200 ms in a field of static white spatial luminance noise (shown) or against a uniform field (no noise; not shown). For measurements in noise, 100 ms of noise preceded and followed the letter presentation.

square checks with luminances drawn randomly from a uniform distribution. Each noise check subtended 0.14° by 0.14°, which corresponds to three noise checks per letter stroke width. The noise spectral density (N) was computed as the product of squared root mean square (rms) contrast and check area.[25] N ranged from 0 to 4.4×10^{-4} deg^2 in five steps, each separated by 0.8 log units.

As illustrated in Figure 1, the letter and noise were presented asynchronously, a procedure used in prior visual noise-based studies.[13,14,25–28] The letter duration was 200 ms, whereas the total noise duration was 400 ms. The letter onset was delayed relative to the noise onset by 100 ms, and 100 ms of noise also followed the letter offset. This mode of stimulus presentation is thought to target the magnocellular visual pathway[22] due to the abrupt onset and offset transients generated by the letter appearing against the static noise field. We sought to target the magnocellular pathway, as this pathway may be more affected than the parvocellular pathway in subjects with XLRS.[8]

Procedure

The subject's task was to identify the letter presented, which was selected at random from the Sloan set. No feedback was given. CS for letter identification was measured using a 10-alternative forced-choice staircase procedure. The staircase started at the maximum possible contrast and then decreased

by 0.3 log units following each correct response until an incorrect response was recorded. After this initial search, log CS was determined using a two-down, one-up decision rule, which provides an estimate of the 76% correct point on a psychometric function.[29] Each staircase continued until 12 reversals had occurred, and the geometric mean of the last four reversals was taken as CS. The order of noise level (N) testing was determined at random for each subject.

Analysis

Data were analyzed using the LAM, as follows: (1) CS measurements were converted to log threshold signal energy (E_t), which was computed as the integral of the squared signal function[25]; (2) log E_t was plotted as a function of log N and the data were fit with the following equation[19]:

$$\log\ E_t = \log(k) + \log\left(N + N_{eq}\right), \qquad (1)$$

where k and N_{eq} were free parameters that were adjusted to minimize the mean squared error between the data and the fit. The subject's equivalent intrinsic noise (N_{eq}) is given directly by Equation 1 and sampling efficiency is reciprocally related to k of Equation 1.[19,30]

Clinical Measurements

Distance visual acuity was measured using a Lighthouse distance visual acuity chart viewed through a phoropter with the subject's optimum correction. Pelli-Robson chart CS was measured from a 1 m test distance using a letter-by-letter scoring rule[31] where each correctly identified letter was assigned a value of 0.05 log units. Retinal thickness was measured with an Optos OCT/SLO/microperimeter (Optos, Dunfermline, UK). The measurements of retinal thickness have been reported for these subjects[20] and are used in the present study for correlations with E_{t0}, N_{eq}, and sampling efficiency. In brief, retinal thickness was measured from the same eye in which the psychophysical measurements were performed. One high-resolution SD-OCT b-scan, comprised of an average of approximately 30 individual scans, was obtained along the horizontal meridian through the fovea. The OCT was segmented using a semi-automated approach[32–34] that was performed in MATLAB using custom-written software. The thicknesses of two layers were quantified: (1) the outer nuclear layer + outer plexiform layer (ONL^+), defined as the distance between the border of the inner nuclear layer/outer plexiform layer and the inner segment ellipsoid; (2) outer segments + RPE (OS^+), defined as the distance between the inner segment ellipsoid and Bruch's membrane/choroid.

The measures of outer retina thickness were compared to E_{t0}, N_{eq}, and sampling efficiency by adopting the structure-function model of Jacobson et al.,[35,36] which was expanded on by Rangaswamy et al.[37] to include combined ONL^+ and OS^+ structure-function measures. In brief, the normalized product of ONL^+ and OS^+ ($ONL^+ \times OS^+$) thickness was computed by dividing each subject's $ONL^+ \times OS^+$ thickness by the mean control $ONL^+ \times OS^+$ thickness. Thickness measurements were averaged over the central macular area (4°) that presumably mediated letter identification. In this model, it is assumed that the number of photoreceptors is proportional to ONL^+ thickness and the OS length is proportional to OS^+ thickness (both measured by OCT).[35–37] Consequently, the product of these measurements should provide a better measure of quantum absorption than either measure alone.[37] The psychophysical measures of E_{t0}, N_{eq}, and sampling efficiency for each subject with XLRS were also normalized by the control mean for comparison to the thickness values.

Results

Figure 2 shows log E_t as a function of log N for the subjects with XLRS (color coding conventions are given in the Table), as well as for the range of control data (gray region). The log CS equivalents of the log E_t values are shown on the right y-axis. The curves are the least-squares best fit of Equation 1 to each subject's

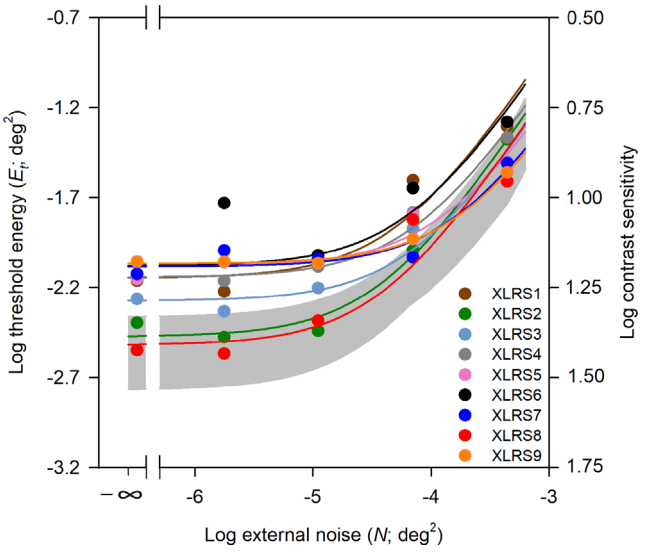

Figure 2. Log E_t as a function of log N for the 9 subjects with XLRS (color coded as shown in the Table) compared with the normal range for the 10 control subjects (*gray region*). The *curves* are the least-squares best fits of Equation 1 to the data of each subject with XLRS. The log CS equivalents of the log E_t values are given on the right *y*-axis.

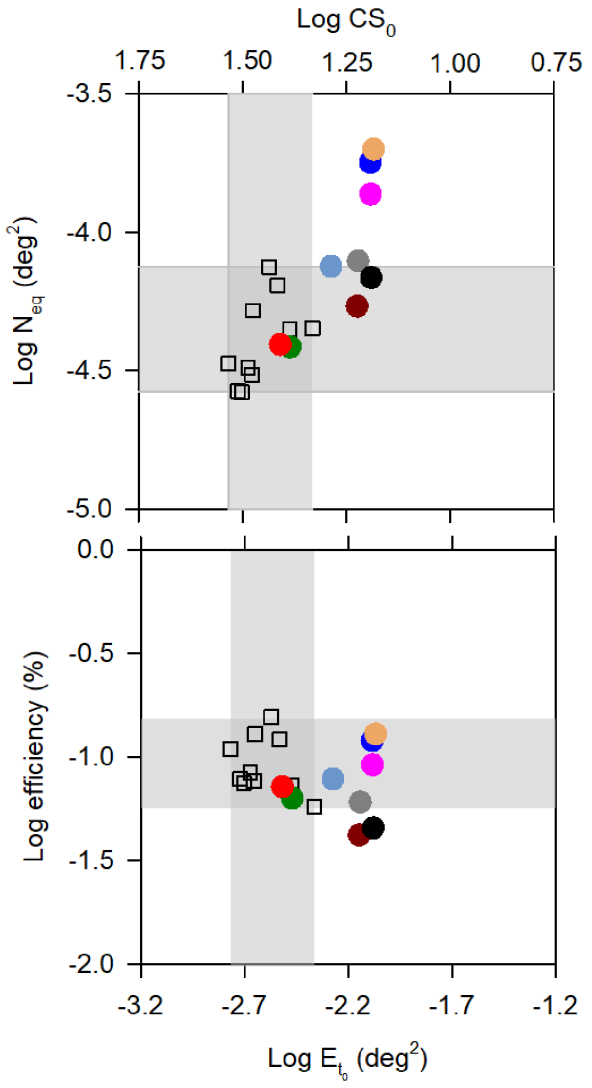

Figure 3. Log N_{eq} versus log E_{t0} (top) and log efficiency versus log E_{t0} (bottom) for the 9 subjects with XLRS and 10 control subjects (*open squares*). The *gray regions* demarcate the normal ranges of log N_{eq} (top; horizontal region), log efficiency (bottom; horizontal region), and E_{t0} (vertical regions). The log CS_0 equivalents (i.e. CS in the absence of noise) of the log E_{t0} values are given on the top x-axis.

data. The values of E_t measured in the absence of noise (E_{t0}; the leftmost points in Fig. 2) varied among the subjects with XLRS (approximately threefold difference among the subjects); seven of the nine subjects with XLRS had E_{t0} that was outside of the control range (CS loss in the absence of noise). In comparison, E_t measured in the highest level of noise (the rightmost points in Fig. 2) was elevated for only two subjects, and the elevations were small.

Figure 3 shows the values of log N_{eq} (top) and log efficiency (bottom) that were derived from the LAM. The log N_{eq} and log efficiency values are plotted as a function of log E_{t0} for the subjects with XLRS (color-coded as in Fig. 2) and for the control subjects (black open squares). The log CS_0 equivalents (contrast sensitivity in the absence of noise) are plotted along the top x-axis. The vertical gray regions demarcate the normal range of E_{t0}, whereas the horizontal gray regions show the normal range of N_{eq} (Fig. 3; top) or efficiency (Fig. 3; bottom). Three subgroups of subjects with XLRS were identified: (1) normal E_{t0} and normal N_{eq} (subjects 2 and 8); (2) elevated E_{t0} (reduced CS_0) and normal/nearly normal N_{eq} (subjects 1, 3, 4, 6); (3) elevated E_{t0} (reduced CS_0) and elevated N_{eq} (subjects 5, 7, 9). The E_{t0} elevation for subgroups 2 and 3 ranged from 0.09 to 0.30 log units above the upper limit of normal. The N_{eq} elevation for subgroup 3 ranged from 0.26 to 0.43 log units above the upper limit of normal. There was a statistically significant correlation between log N_{eq} and log E_{t0} for the subjects with XLRS ($r = 0.78$, $P = 0.01$), but not for the control subjects ($r = 0.56$, $P = 0.09$). T-tests were performed to compare the values of log N_{eq} and log E_{t0} between the control and XLRS subject groups. The t-tests indicated significant elevations in log E_{t0} ($t = 3.08$, $P = 0.007$) and log N_{eq} ($t = 5.83$, $P < 0.001$) for the subjects with XLRS. The efficiency values for the subjects with XLRS (Fig. 3; bottom) were generally within the range of normal, with the exception of subjects 1 and 6 who had small efficiency losses (less than 2%). A t-test indicated that log efficiency for the XLRS group was not significantly different from that of the control group ($t = 1.42$, $P = 0.17$). Log efficiency was not significantly correlated with log E_{t0} for the subjects with XLRS ($r = 0.19$, $P = 0.63$) or for the controls ($r = -0.27$, $P = 0.46$).

Figure 3 shows that the CS_0 losses were generally modest for the subjects with XLRS. Nevertheless, the mean CS_0 for the subjects with XLRS (1.25) was significantly lower ($t = 5.83$, $P < 0.001$) than that of the control subjects (1.45). The CS_0 abnormality was somewhat greater than the Pelli-Robson CS chart abnormality (Table). Specifically, Pelli-Robson CS was reduced (less than 1.8) for five of the nine subjects with XLRS. However, the losses were small. Overall, the mean Pelli-Robson CS for the subjects with XLRS (1.80) was significantly lower ($t = 3.39$, $P = 0.04$) than that of the control subjects (1.90).

Figure 4 shows the relationship between outer retina thickness and threshold elevation (E_{t0}; top), N_{eq} elevation (middle), and efficiency loss (bottom) for each subject with XLRS and for the controls (gray regions). The dashed lines represent the linear model described above that predicts that normalized $ONL^+ \times OS^+$ thickness is linearly related to E_{t0} elevation, N_{eq} elevation, and efficiency loss. This model has been translated vertically and horizontally to capture the normal

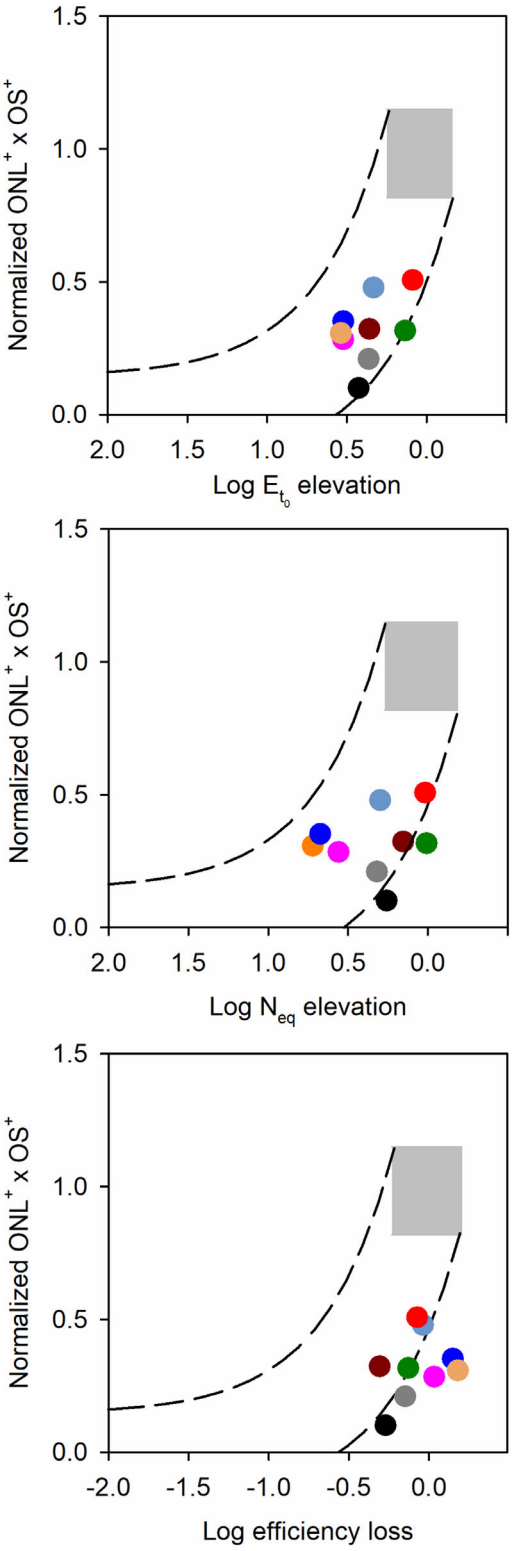

Figure 4. Normalized ONL$^+$ x OS$^+$ thickness is plotted as a function of log E_{t0} elevation (top), N_{eq} elevation (middle), and log efficiency loss (bottom). Data are shown for each subject with XLRS and the *gray regions* represent the normal ranges. The *dashed lines* represent the prediction of the linear model as described in the text, which has been translated vertically and horizontally to capture the normal variability.

variability marked by the control range (gray boxes). The top panel of Figure 4 shows that the data for all of the subjects with XLRS fell within the dashed lines predicted by the model. However, the correlation between ONL$^+$ × OS$^+$ thickness and log E_{t0} elevation did not achieve statistical significance (Spearman's $\rho = 0.55$, $P = 0.11$). Outer-retinal thickness was reduced considerably in all of the subjects with XLRS, but the threshold elevations were often modest in comparison. For example, subjects 2 and 8 had E_{t0} within the normal range, despite approximately 50% thinning of the ONL$^+$ × OS$^+$. Other subjects with XLRS (e.g., subjects 5, 7, 9) had thinning that was approximately proportional to their E_{t0} elevation. The middle panel of Figure 4 shows that the measurements of thickness and N_{eq} elevation fell into the range predicted by the model for seven of the nine subjects with XLRS. The exceptions were subjects 2 and 6 who had slightly better N_{eq} than predicted by their outer retinal thickness. The correlation between ONL$^+$ × OS$^+$ thickness and N_{eq} was weak (Spearman's $\rho = 0.25$, $P = 0.49$). The bottom panel of Figure 4 shows that the thickness and efficiency loss data fell into the range predicted by the model for four of the nine subjects with XLRS. In general, the subjects had little or no efficiency loss, despite outer retinal thinning. The correlation between ONL$^+$ × OS$^+$ thickness and efficiency loss was weak (Spearman's $\rho = 0.25$, $P = 0.49$).

Discussion

This study determined the relationships among CS, internal noise, and sampling efficiency, as well as how these three psychophysical parameters relate to outer retinal thickness, in subjects with XLRS. The primary findings in our cohort of XLRS subjects are that (1) all subjects with elevated internal noise had reduced CS, but not all subjects with XLRS had internal noise elevation or CS loss; (2) sampling efficiency was normal or slightly reduced in subjects with XLRS; (3) a linear model that relates outer-retina structure and CS, as well as outer-retina structure and internal noise, may be useful for describing structure-function relationships in subjects with XLRS.

CS was abnormally low in seven of the nine subjects with XLRS, but the CS losses tended to be modest (mean reduction of 0.16 log units below the lower limit of normal; a factor of 1.46). There was a significant correlation between internal noise and CS, such that subjects with the highest internal noise tended to have lowest CS. Indeed, all of our subjects with elevated N_{eq} had reduced CS. However, there was a subgroup

of subjects who had low CS, but internal noise within the range of normal or nearly normal (subjects 1, 3, 4, 6). For these subjects, low efficiency may have contributed to their low CS. The small sample size, which is a limitation of the present study, precludes determining whether there are clear subgroups of subjects with XLRS who have efficiency losses that affect CS alone or in combination with N_{eq}. Nevertheless, the data do show that only internal noise is correlated with CS and that efficiency losses, when present, were within 2% of the lower limit of normal in our cohort.

The CS losses assessed with the computer-implemented noise-based protocol somewhat exceeded the CS losses measured with the Pelli-Robson CS chart in this sample of subjects with XLRS. Overall, the extent of CS loss is consistent previous work that also showed generally small losses for measurements made with large letter targets.[7,8] Differences between CS measured with the noise-based protocol and with the Pelli-Robson chart could be attributed to stimulus duration (200 ms for the CS_0 measurements and unlimited duration for the Pelli-Robson chart measurements) or greater sensitivity of the noise-based protocol due to the video display's ability to produce fine contrast steps. The size of the letter used in the present study (1.4 log MAR) is similar to that of the Pelli-Robson chart tested at 1 m (1.5 log MAR). Given that letter CS is approximately independent of size for letters larger than 1.4 log MAR,[38] the somewhat greater CS loss for the CS_0 measurements can more likely be attributed to the brief stimulus duration or to the enhanced sensitivity of the video display. Assessment of temporal integration in subjects with XLRS would be of interest in future studies to evaluate this hypothesis. It would also be of interest to examine CS using letters that are smaller than those used in the present report. Previous work has shown that CS losses are more apparent with high spatial frequency gratings (equivalent to small letters) than for low spatial frequency gratings (equivalent to large letters) in subjects with XLRS. Indeed, the modest CS losses in this sample of XLRS subjects is a limitation of the present study. The use of smaller targets may expand the range of CS, which could improve the predictive power of the modeling. However, the use of small letters, particularly those near the acuity limit, could confound CS measures due to the subjects' VA losses. In the present study, the 1.4 log MAR letter was approximately 5x larger than the VA limit of subject 2 who had the worst VA of the sample (0.68 log MAR). As such, there is little concern that VA loss significantly affected CS measurements in the present study. Furthermore, there was no significant correlation between CS_0 and log MAR VA ($r = -0.19$, $P = 0.62$) or between Pelli-Robson CS and log MAR VA ($r = -0.42$, $P = 0.26$) in the present study. The lack of correlation between large letter CS and VA has been reported previously in subjects with XLRS.[8] It would be of interest to examine CS across a range of letter sizes in future work, which could provide a more comprehensive understanding of CS loss and internal nose elevation in subjects with XLRS.

As noted in the Introduction, elevated retinal "noise" has been reported in a mouse model of XLRS. Single-cell RGC electrophysiology in young *Rs1* mutant mice demonstrated elevated spiking activity in the absence of visual stimulation and a reduced signal-to-noise ratio in response to light stimuli.[12] Superficially, this finding is consistent with the present report, which showed that high levels of internal noise are associated with low CS. However, the extent to which elevated intrinsic noise in subjects with XLRS is a behavioral manifestation of physiologic RGC noise is unclear. Furthermore, we do not know whether elevated RGC activity persists in *Rs1* mutant mice at later ages, which would better match this cohort of subjects with XLRS. Further work to link psychophysical noise in humans with physiological RGC noise could open new avenues for potential treatments, as recent work has shown that physiological RGC noise can be reduced by inhibiting the retinoic acid receptor, which, in turn, improves behavioral light sensitivity in mice with retinal degeneration.[39] Alternatively, low CS in subjects with XLRS may be due to nonlinear processes, such as a gain abnormality, rather than noise.[40] An important limitation of the LAM is the assumption that contrast processing is linear and that noise is additive. If the assumption of linearity does not hold, then elevations in N_{eq} could be due entirely, or in part, to abnormal retinal nonlinearities in subjects with XLRS.

A simple linear model was adopted from prior research[35–37] to examine structure-function associations in subjects with XLRS. Data from all of the subjects with XLRS fell within the model predictions, suggesting that outer retinal thinning may account for the E_{to} elevation (CS_0 loss) in our sample of subjects with XLRS. Given the extent of E_{to} elevation discussed above, data for our XLRS subjects primarily fell within the descending region of the model prediction, as shown in Figure 4. That is, our XLRS subjects all had considerable outer retinal thinning (reductions of at least ±50% of normal) and threshold elevations of 0.6 log units (factor of four) or less, relative to the normal mean. Nevertheless, the correlation between outer retina thickness and E_{to} elevation was not significant. This is, in part, because some subjects had E_{to}

elevation that was similar to their extent of retinal thinning (subjects 5, 7, 9), whereas others had marked thinning, but normal or moderately elevated E_{to}. A previous study in these nine subjects that assessed outer retinal thinning and threshold elevation using small (0.43 deg; Goldmann III) stimuli showed a significant correlation between normalized $ONL^{+} \times OS^{+}$ thickness and threshold elevation. In that study, these subjects had considerably larger threshold elevations (some exceeding 2 log units). A similar pattern was observed for the relationship between outer-retinal thickness and N_{eq} (Fig. 4; middle): data for the subjects with XLRS primarily fell within the descending region of the model, and 7/9 subjects were within the limits of the model prediction. The correlation between outer retina thickness and N_{eq} elevation was not significant. As observed for the E_{to} measurements, this is likely due to some subjects having N_{eq} elevation that was similar to their extent of retinal thinning (subjects 5, 7, 9), whereas others had marked thinning, but normal or minimally elevated N_{eq}. The pattern for efficiency was somewhat different (Fig. 4; bottom) in that only 4/9 subjects were within the limits of the model prediction. This is because our subjects with XLRS generally had normal efficiency, despite their considerable outer-retina thinning. Thus, the linear model accounted reasonably well for the E_{to} and N_{eq} measurements, but not for efficiency measurements. Of note, there were no apparent relationships between the subjects' genotypes and their psychophysical or structural measurements, but the small sample size makes genotype-phenotype associations uncertain. There was also no apparent association with the total retinal thickness and E_{to}, N_{eq} or efficiency. Some subjects (e.g., subject 2) had total retinal thickness that was more than 2.5 times larger than normal because of large foveal cystic spaces, but E_{to}, N_{eq}, and efficiency were within the range of normal. This suggests that cystic spaces alone may not markedly affect visual function, consistent with prior reports that found no association with cyst volume and visual acuity.[7]

In conclusion, the results indicate that increased intrinsic noise within the visual pathway may be a determinant of CS impairments in some subjects with XLRS. Their CS losses for large letters, however, were less than what may be predicted on the basis of their sensitivity measured with small spots of light[20] or high frequency sinewave gratings.[8] Future investigations to link psychophysical noise elevations in human subjects with XLRS and physiological noise elevations in animal models of XLRS could provide an intriguing line of work with translational potential.

Acknowledgments

The authors thank Neal Peachey for comments on the manuscript.

Supported by the National Institutes of Health R01EY029796 (J.J.M.), P30EY001792 (UIC DOVS), K12EY021475 (R.A.H.); The Pangere Family Foundation (G.A.F.); unrestricted funds from Research to Prevent Blindness (UIC DOVS).

Disclosure: **J.J. McAnany,** None; **J.C. Park,** None; **G.A. Fishman,** None; **R.A. Hyde,** None

References

1. Sikkink SK, Biswas S, Parry NR, Stanga PE, Trump D. X-linked retinoschisis: an update. *J Med Genet.* 2007;44:225–232.
2. Sauer CG, Gehrig A, Warneke-Wittstock R, et al. Positional cloning of the gene associated with X-linked juvenile retinoschisis. *Nat Genet.* 1997;17:164–170.
3. Sieving PA, MacDonald IM, Chan S. X-Linked Juvenile Retinoschisis. In: Adam MP, Ardinger HH, Pagon RA, et al. (eds), *GeneReviews((R)).* Seattle (WA): GeneReviews; 1993.
4. Wang T, Zhou A, Waters CT, O'Connor E, Read RJ, Trump D. Molecular pathology of X linked retinoschisis: mutations interfere with retinoschisin secretion and oligomerisation. *Br J Ophthalmol.* 2006;90:81–86.
5. Bennett LD, Wang YZ, Klein M, Pennesi ME, Jayasundera T, Birch DG. Structure/Psychophysical Relationships in X-Linked Retinoschisis. *Invest Ophthalmol Vis Sci.* 2016;57:332–337.
6. Tantri A, Vrabec TR, Cu-Unjieng A, Frost A, Annesley WH, Donoso LA. X-linked retinoschisis: a clinical and molecular genetic review. *Surv Ophthalmol.* 2004;49:214–230.
7. Pennesi ME, Birch DG, Jayasundera KT, et al. Prospective Evaluation of Patients With X-Linked Retinoschisis During 18 Months. *Invest Ophthalmol Vis Sci.* 2018;59:5941–5956.
8. Alexander KR, Barnes CS, Fishman GA. Characteristics of contrast processing deficits in X-linked retinoschisis. *Vision Res.* 2005;45:2095–2107.
9. West SK, Rubin GS, Broman AT, Munoz B, Bandeen-Roche K, Turano K. How does visual

impairment affect performance on tasks of everyday life? The SEE Project. Salisbury Eye Evaluation. *Arch Ophthalmol.* 2002;120:774–780.
10. Szlyk JP, Seiple W, Fishman GA, Alexander KR, Grover S, Mahler CL. Perceived and actual performance of daily tasks: relationship to visual function tests in individuals with retinitis pigmentosa. *Ophthalmology.* 2001;108:65–75.
11. McAnany JJ, Park JC, Fishman GA, Collison FT. Full-field electroretinography, pupillometry, and luminance thresholds in X-linked retinoschisis. *Invest Ophthalmol Vis Sci.* 2020;61:53.
12. Liu Y, Kinoshita J, Ivanova E, et al. Mouse models of X-linked juvenile retinoschisis have an early onset phenotype, the severity of which varies with genotype. *Hum Mol Genet.* 2019;28:3072–3090.
13. Pelli DG, Levi DM, ST Chung. Using visual noise to characterize amblyopic letter identification. *J Vis.* 2004;4:904–920.
14. McAnany JJ, Alexander KR, Genead MA, Fishman GA. Equivalent intrinsic noise, sampling efficiency, and contrast sensitivity in patients with retinitis pigmentosa. *Invest Ophthalmol Vis Sci.* 2013;54:3857–3862.
15. McAnany JJ, Park JC. Reduced contrast sensitivity is associated with elevated equivalent intrinsic noise in type 2 diabetics who have mild or no retinopathy. *Invest Ophthalmol Vis Sci.* 2018;59:2652–2658.
16. Kersten D, Plant GT. Assessing contrast sensitivity behind cloudy media. *Clin Vis Sci.* 1988;2:143–158.
17. Huang CB, Lu ZL, Zhou Y. Mechanisms underlying perceptual learning of contrast detection in adults with anisometropic amblyopia. *J Vis.* 2009;9:24, 21-14.
18. Levi DM, Klein SA, Chen I. What limits performance in the amblyopic visual system: seeing signals in noise with an amblyopic brain. *J Vis.* 2008;8(4):1.1–1.23.
19. Pelli DG, Farell B. Why use noise? *J Opt Soc Am A Opt Image Sci Vis.* 1999;16:647–653.
20. McAnany JJ, Park JC, Fishman GA, Hyde RA. Luminance Thresholds and Their Correlation With Retinal Structure in X-Linked Retinoschisis. *Invest Ophthalmol Vis Sci.* 2021;62:25.
21. Hall C, Wang S, Bhagat R, McAnany JJ. Effect of luminance noise on the object frequencies mediating letter identification. *Front Psychol.* 2014;5:663.
22. Hall CM, McAnany JJ. Luminance noise as a novel approach for measuring contrast sensitivity within the magnocellular and parvocellular pathways. *J Vis.* 2017;17:5.
23. Recommended standard procedures for the clinical measurement and specification of visual acuity. Report of working group 39. Committee on vision. Assembly of Behavioral and Social Sciences, National Research Council, National Academy of Sciences, Washington, D.C. *Adv Ophthalmol.* 1980;41:103–148.
24. Hall C, Wang S, McAnany JJ. Individual letter contrast thresholds: effect of object frequency and noise. *Optom Vis Sci.* 2015;92:1125–1132.
25. Legge GE, Kersten D, Burgess AE. Contrast discrimination in noise. *J Opt Soc Am A.* 1987;4:391–404.
26. Manahilov V, Calvert J, Simpson WA. Temporal properties of the visual responses to luminance and contrast modulated noise. *Vision Res.* 2003;43:1855–1867.
27. McAnany JJ, Alexander KR. Contrast thresholds in additive luminance noise: effect of noise temporal characteristics. *Vision Res.* 2009;49:1389–1396.
28. McAnany JJ, Alexander KR. Spatial contrast sensitivity in dynamic and static additive luminance noise. *Vision Res.* 2010;50:1957–1965.
29. Garcia-Perez MA. Forced-choice staircases with fixed step sizes: asymptotic and small-sample properties. *Vision Res.* 1998;38:1861–1881.
30. Pelli DG, Burns CW, Farell B, Moore-Page DC. Feature detection and letter identification. *Vision Res.* 2006;46:4646–4674.
31. Elliott DB, Bullimore MA, Bailey IL. Improving the reliability of the Pelli-Robson contrast sensitivity test. *Clin Vis Sci.* 1991;6:471–475.
32. Hood DC, Cho J, Raza AS, Dale EA, Wang M. Reliability of a computer-aided manual procedure for segmenting optical coherence tomography scans. *Optom Vis Sci.* 2011;88:113–123.
33. McAnany JJ, Park JC, Liu K, et al. Contrast sensitivity is associated with outer-retina thickness in early-stage diabetic retinopathy. *Acta Ophthalmol.* 2020;98:e224–e231.
34. Park JC, Chen YF, Liu M, Liu K, McAnany JJ. Structural and functional abnormalities in early-stage diabetic retinopathy. *Curr Eye Res.* 2020;45:975–985.
35. Jacobson SG, Aleman TS, Cideciyan AV, et al. Identifying photoreceptors in blind eyes caused by RPE65 mutations: prerequisite for human gene therapy success. *Proc Natl Acad Sci USA.* 2005;102:6177–6182.
36. Jacobson SG, Cideciyan AV, Aleman TS, et al. Usher syndromes due to MYO7A, PCDH15, USH2A or GPR98 mutations share retinal disease mechanism. *Hum Mol Genet.* 2008;17:2405–2415.

37. Rangaswamy NV, Patel HM, Locke KG, Hood DC, Birch DG. A comparison of visual field sensitivity to photoreceptor thickness in retinitis pigmentosa. *Invest Ophthalmol Vis Sci.* 2010;51:4213–4219.
38. McAnany JJ, Alexander KR. Contrast sensitivity for letter optotypes vs. gratings under conditions biased toward parvocellular and magnocellular pathways. *Vision Res.* 2006;46:1574–1584.
39. Telias M, Denlinger B, Helft Z, Thornton C, Beckwith-Cohen B, Kramer RH. Retinoic acid induces hyperactivity, and blocking its receptor unmasks light responses and augments vision in retinal degeneration. *Neuron.* 2019;102:574–586.e575.
40. Baldwin AS, Baker DH, Hess RF. What do contrast threshold equivalent noise studies actually measure? Noise vs. nonlinearity in different masking paradigms. *PLoS One.* 2016;11:e0150942.